JOURNAL OF Materials CHEMISTRY

Combustion synthesis of nanometal particles supported on α-Al_2O_3: CO oxidation and NO reduction catalysts

Parthasarathi Bera,[a] K. C. Patil,[b] V. Jayaram,[a] M. S. Hegde*[a] and G. N. Subbanna[c]

[a]*Solid State and Structural Chemistry Unit, Indian Institute of Science, Bangalore-560012, India. E-mail: mshegde@sscu.iisc.ernet.in*
[b]*Department of Inorganic and Physical Chemistry, Indian Institute of Science, Bangalore-560012, India*
[c]*Materials Research Centre, Indian Institute of Science, Bangalore-560012, India*

Received 9th March 1999, Accepted 25th May 1999

Nanoparticles of Pt, Pd, Ag and Au supported on α-Al_2O_3 have been synthesized by the combustion method for the first time and characterized by X-ray diffraction, transmission electron microscopy and X-ray photoelectron spectroscopy. Catalytic activities of these nanosized materials have been investigated. For the $CO+O_2$ reaction, 100% CO conversion occurs below 300 °C over supported Pt, Pd and Ag metals whereas 90% conversion is observed over Au at 450 °C. Similarly 100% NO conversion is seen over 1% Pd/Al_2O_3 and 1% Pt/Al_2O_3 below 400 °C for the NO + CO reaction whereas ≈90% NO is converted into N_2 above 650 °C on 1% Ag/Al_2O_3 and 1% Au/Al_2O_3.

Introduction

Ultra-fine metal particles as a distinct state of matter are of interest due to their structure and reactivity. The study of nanomaterials is of interest to chemists, physicists and material scientists. The size dependent reactivity and catalytic properties of metal nanoparticles have been investigated.[1–6] The catalytic properties of small metal particles differ widely depending on the particle size. These small metal particles are highly reactive and undergo agglomeration which limits their application in the field of catalysis. However, they can be stabilized in suitable solid matrices such as alumina, ceria, zirconia, titania, silica and zeolites for subsequent use in heterogeneous catalysis.

Recently, supported metal catalysts have attracted much attention because of their high catalytic activity for NO reduction, CO oxidation, CO hydrogenation and CH_3OH synthesis.[7–14] These catalysts are usually prepared by impregnation, ion exchange, anchoring/grafting, spreading and wetting, hydrolysis and homogeneous decomposition–precipitation.[15] There has been a new trend regarding novel chemical routes of synthesis which can lead to ultra-fine, high surface area catalysts for heterogeneous catalysis. Some of these methods are: sol–gel, aerosol, coprecipitation and solution combustion. Haruta *et al.*[16,17] have prepared supported gold catalysts by coprecipitation which show CO oxidation below 0 °C.

Pt, Pd, Ag and Au salts are known to decompose to the respective metals at relatively low temperature (< 500 °C) and therefore we considered it worthwhile to see if these metal particles can be dispersed on α-Al_2O_3 by the combustion method. Here, we report for the first time a combustion route to synthesize fine Pt, Pd, Ag and Au metal particles supported on α-Al_2O_3. These fine and high surface area materials formed *in situ* have been found to be good CO oxidation and NO reduction catalysts.

Experimental

Synthesis

The combustion mixture for the preparation of 1% Pt/Al_2O_3 contained $Al(NO_3)_3$, H_2PtCl_6 and NH_2CONH_2 (urea) in the mole ratio 1.98 : 0.02 : 4.95. In a typical preparation, 8.5 g of $Al(NO_3)_3$ (Glaxo India Ltd., 99.9%), 0.1182 g of H_2PtCl_6 (Ranbaxy Laboratories Ltd., 99%) and 3.3992 g of NH_2CONH_2 (Glaxo India Ltd., 99%) were dissolved in the minimum volume of water in a borosilicate dish of 130 cm^3 capacity. The dish containing the redox mixture was introduced into a muffle furnace ($l=28$ cm, $b=17$ cm, $h=9$ cm) maintained at 500 °C. Initially the solution boiled with frothing and foaming and underwent dehydration. At the point of complete dehydration, the surface foam ignited, burning with a flame (≈1500 °C) and yielding a voluminous solid product within 5 min. Similarly, 0.5% Pt, 1% Pd, 1% Ag and 1% Au metals dispersed on α-Al_2O_3 have been prepared. In case of Pd, Ag and Au the precursors used were $PdCl_2$ (Glaxo India Ltd., 99%), $AgNO_3$ (E. Merck India Ltd., 99.9%) and $HAuCl_4$ (Avis Chemica, 99%) respectively. Pt/Al_2O_3 and Pd/Al_2O_3 samples are grayish, Ag/Al_2O_3 is brown and Au/Al_2O_3 is magenta.

Characterization

Combustion derived metal/Al_2O_3 products were characterized by their powder X-ray diffraction (XRD), transmission electron microscopy (TEM), powder density, particle size measurement and X-ray photoelectron spectroscopy (XPS). The X-ray diffraction patterns of the products were recorded on a JEOL JDX-8P diffractometer using Cu-Kα radiation with a Ni filter and scan rate of 2° min^{-1}. TEM of powders was carried out using a JEOL JEM-200CX transmission electron microscope operated at 200 kV. Particle size analysis was carried out using a particle size analyzer (Malvern Instruments Ltd., UK) based on the light scattering principle and employing the sedimentation technique. X-Ray photoelectron spectra of these supported metal particles were recorded in an ESCA-3 Mark II spectrometer (VG Scientific Limited, UK) using Al-Kα radiation. Binding energies calibrated with respect to C (1s) at 285 eV were accurate within ±0.2 eV.

Adsorption studies

Adsorption of CO on 1% Pt/Al_2O_3, 1% Pd/Al_2O_3 and Al_2O_3 was carried out in a constant volume glass system. Typically 0.5 g of the catalyst was degassed at 250 °C in a vacuum system (10^{-6} Torr) for 3 h, then cooled to 0 °C. A known volume of CO was passed into the sample tube and the pressure measured by a digital high pressure pirani gauge calibrated against N_2. The volume of CO adsorbed expressed in cm^3 (STP) was accurate within ±15%.

Temperature programmed reaction (TPR)

Gas–solid reactions were carried out in a temperature programmed reaction system equipped with a quadrupole mass spectrometer QXK 300 (VG Scientific Ltd., UK) for product analysis. The details of this home-made TPR set-up have been described elsewhere.[18] Typically 0.1–0.2 g of the sample was loaded in a quartz tube reactor of 20 cm length and 6 mm diameter. The reactor was heated from 30 to 750 °C at a rate of 15 °C min^{-1} and the sample temperature measured by a fine chromel–alumel thermocouple immersed in the catalyst. The quartz tube was evacuated to 10^{-6} Torr. The gaseous products were sampled through a fine control leak valve to an ultra high vacuum (UHV) system housing the quadrupole mass spectrometer at 10^{-9} Torr. The gases were passed over the catalysts at a flow rate of 25 μmol s^{-1} and the flow rate was varied from 10 to 30 μmol s^{-1}. Generally, the gas hourly space velocity (GHSV) and the catalyst weight to gas flow rate ratio (W/F) are in the ranges of 30000–90000 h^{-1} and 8.3×10^{-5} to 2.5×10^{-4} g h cm^{-3} respectively. The dynamic pressure of CO for example was in the range 300–500 mTorr in the reaction system in most of the experiments. All the masses were scanned every 10 s. At the end of the reaction the intensity of each mass as a function of temperature (thermogram) was generated. NO, CO and O_2 gases were obtained from Bhoruka Gases Limited, Bangalore. Their purities were better than 99% as analysed by the quadrupole mass spectrometer.

Results and discussion

The formation of metal particles supported on α-Al_2O_3 is confirmed by their characteristic XRD patterns. Typical XRD patterns of as prepared Pt, Pd, Ag and Au supported on α-Al_2O_3 are shown in Fig. 1. In addition to diffraction lines due to α-Al_2O_3, broad peaks of Pt, Pd, Ag and Au are observed. Peaks corresponding to these metal oxides are not observed in any of the products. The crystallite sizes of Pt, Pd Ag and Au metal particles calculated from the Debye–Scherrer equation are 12, 15, 25 and 20 nm respectively. The ring patterns from electron diffraction were analysed and could be indexed to α-Al_2O_3 and the metal (M = Pt, Pd, Ag or Au) particles. The XRD and TEM studies confirm the presence of dispersed metal particles on the support. The morphology of the particles from TEM (1% Pt/Al_2O_3 and 1% Pd/Al_2O_3) is shown in Fig. 2. The combustion yields nearly spherical particles of uniform size. The particle sizes of Pt, Pd Ag and Au metals

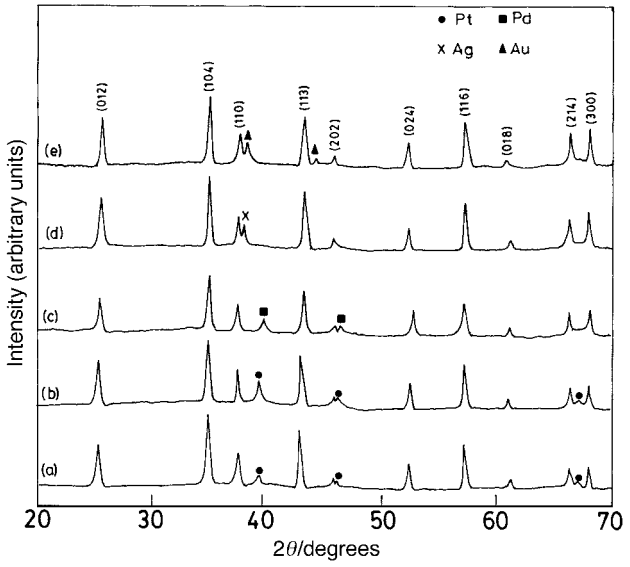

Fig. 1 XRD patterns of (a) 0.5% Pt/Al_2O_3, (b) 1% Pt/Al_2O_3, (c) 1% Pd/Al_2O_3, (d) 1% Ag/Al_2O_3 and (e) 1% Au/Al_2O_3.

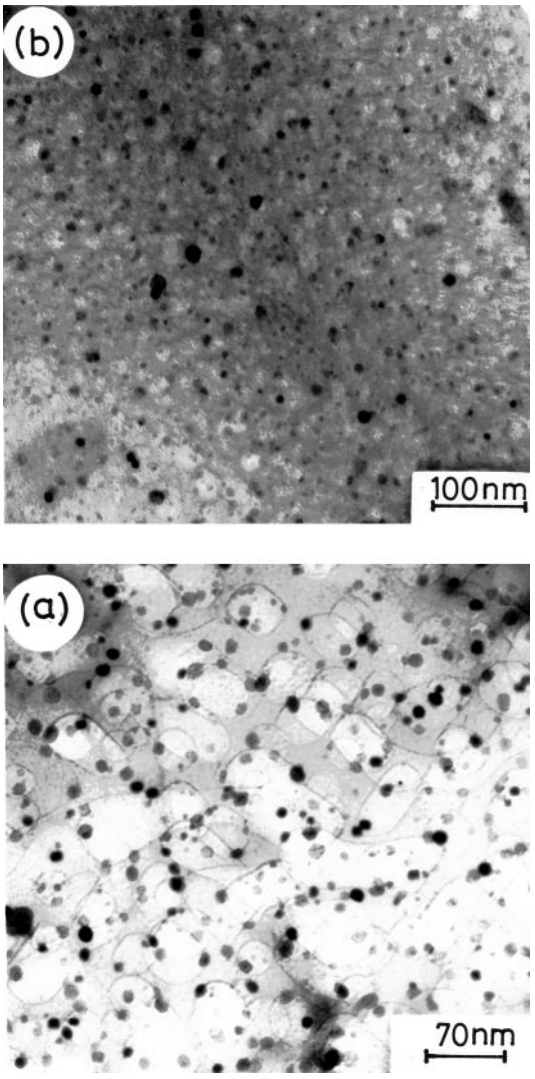

Fig. 2 TEM of (a) 1% Pt/Al_2O_3 and (b) 1% Pd/Al_2O_3. Black dots indicate metal particles.

calculated from TEM are 7, 12, 20 and 15 nm respectively which are close to the values obtained from the XRD study. A typical histogram from TEM of Pt particles dispersed on α-Al_2O_3 is shown in Fig. 3(a). The powder densities of these materials are 80–90% of the theoretical density of α-Al_2O_3. A typical particle size distribution curve of 1% Pt/Al_2O_3 is shown in Fig. 3(b) having a mean size of 35 μm.

M/Al_2O_3 (M = Pt, Pd, Ag or Au) powder samples were made into pellets and core level spectra of Al (2p), O (1s) and the metals were recorded by XPS. In all the samples the Al (2p) peak centered at 74.1 ± 0.1 eV corresponds to Al_2O_3. In general, core level peaks of metals were weak because of very low concentration. Ag (3d) and Au (4f) spectra for Ag/Al_2O_3 and Au/Al_2O_3 are given in the Fig. 4(a) and 4(b) respectively. Binding energies of Ag ($3d_{5/2}$) at 368 eV and Au ($4f_{7/2}$) at 84 eV indeed confirm the presence of the respective metal particles on Al_2O_3. The broadening of core levels is primarily due to nano-metal particles.[19] Pt (4f) peaks overlap with Al (2p) levels and hence Pt metal peaks couldn't be discerned. Pd (3d) metal peaks were also observed similar to Ag (3d) peaks on Al_2O_3.

Adsorption isotherms of CO over 1% Pt/Al_2O_3 and 1% Pd/Al_2O_3 at 0 °C are given in Fig. 5(a) and 5(b) respectively. The isotherms follow Freundlich type adsorption. Assuming monolayer coverage of CO over Pt particles on Al_2O_3, the particle size of Pt calculated from the volume adsorbed per g of the catalyst is 12 ± 2 nm, close to the values obtained from XRD and TEM studies. The particle size of Pd calculated

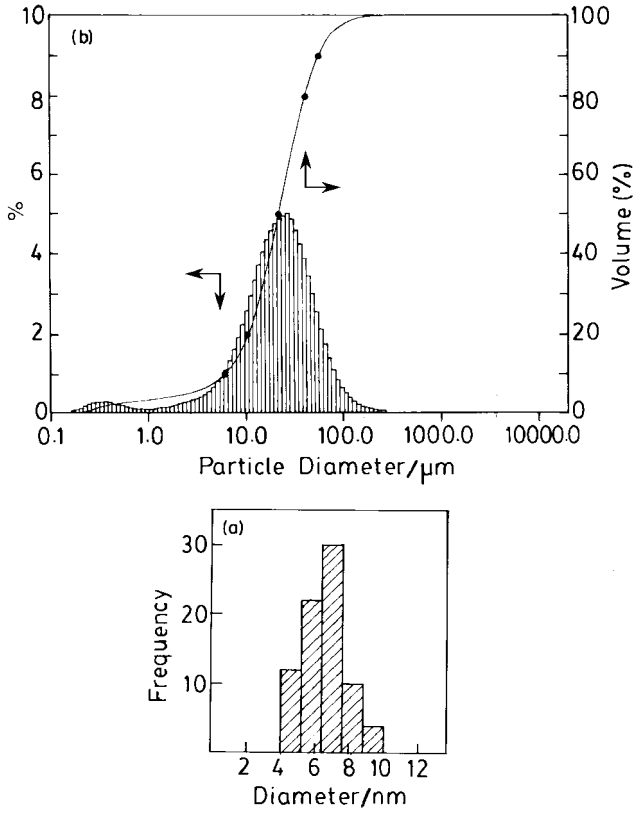

Fig. 3 (a) Particle size histogram of Pt particles in 1% Pt/Al_2O_3 from TEM and (b) particle size distribution curve of 1% Pt/Al_2O_3 from particle size measurement.

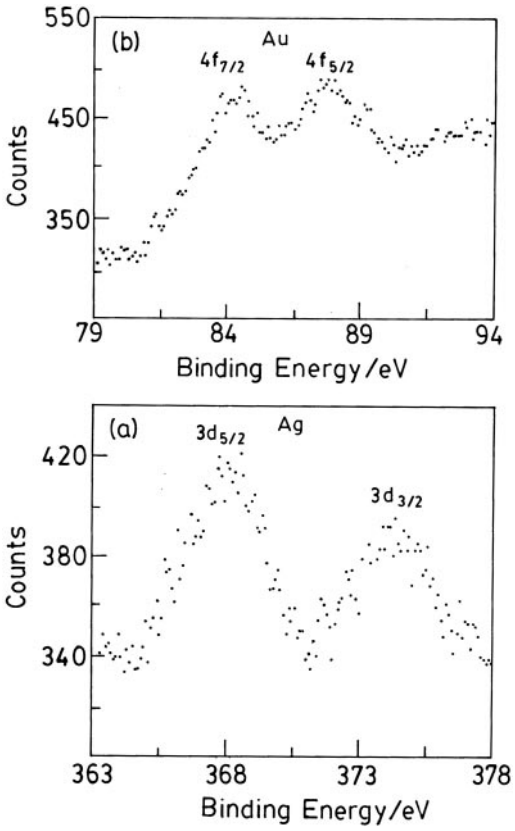

Fig. 4 XPS of (a) Ag (3d) and (b) Au (4f) core levels from metal particles in 1% Ag/Al_2O_3 and 1% Au/Al_2O_3 respectively.

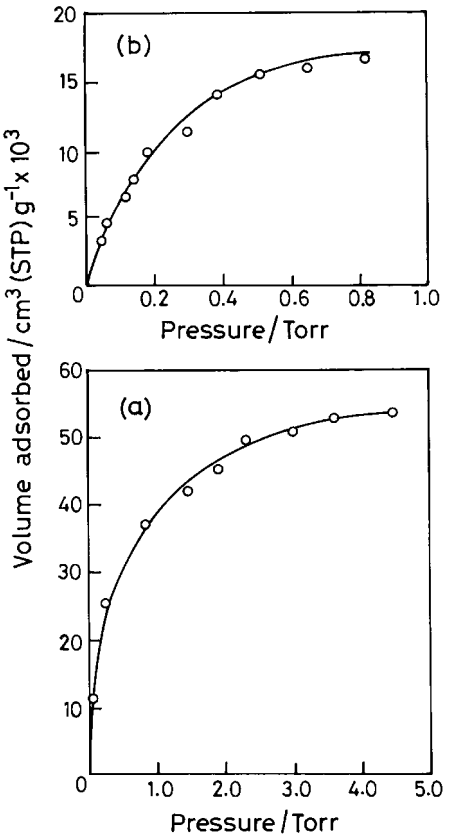

Fig. 5 Adsorption isotherms of CO on (a) 1% Pt/Al_2O_3 and (b) 1% Pd/Al_2O_3 at 0 °C.

from CO adsorption studies is 35 ± 5 nm, about twice the size obtained from the XRD study. Pure Al_2O_3 does not show CO adsorption at 0 °C. Thus, the results clearly demonstrate that CO adsorption over Pt/Al_2O_3 and Pd/Al_2O_3 is due to fine Pt and Pd particles.

Combustion of an aluminium nitrate–urea redox mixture (AN : U = 2 : 5) is known[20] to give micron sized, large surface area (8 m^2 g^{-1}) α-Al_2O_3 within a few minutes. Assuming complete combustion, the formation of α-Al_2O_3 is written as follows:

$$2Al(NO_3)_3\,(aq) + 5NH_2CONH_2\,(aq) \rightarrow Al_2O_3(s) + 5CO_2(g) + 10H_2O(g) + 8N_2(g) \quad (1)$$

The redox mixtures containing AN–U and noble metal salts on combustion yield metal dispersed over alumina. The metal salts pyrolyse to give homogeneously dispersed metals on α-Al_2O_3 formed *in situ*. The high exothermicity of the redox reaction is responsible for the decomposition of the metal salts which are known to yield corresponding metals below 500 °C. Possible reactions occurring during combustion are as follows:

$$H_2PtCl_6 \rightarrow Pt + 2HCl + 2Cl_2 \quad (2)$$

$$PdCl_2 \rightarrow Pd + Cl_2 \quad (3)$$

$$2AgNO_3 \rightarrow 2Ag + 2NO_2 + O_2 \quad (4)$$

$$2HAuCl_4 \rightarrow 2Au + 2HCl + 3Cl_2 \quad (5)$$

Catalytic properties

Catalytic properties of these M/Al_2O_3 materials have been investigated for CO oxidation and NO reduction by CO. The CO oxidation was carried out over supported metal particles in the presence of oxygen. Typical temperature profiles of reactants and product for the $CO + O_2$ reaction over 1% Pt/Al_2O_3 are shown in Fig. 6. A sharp decrease in CO concen-

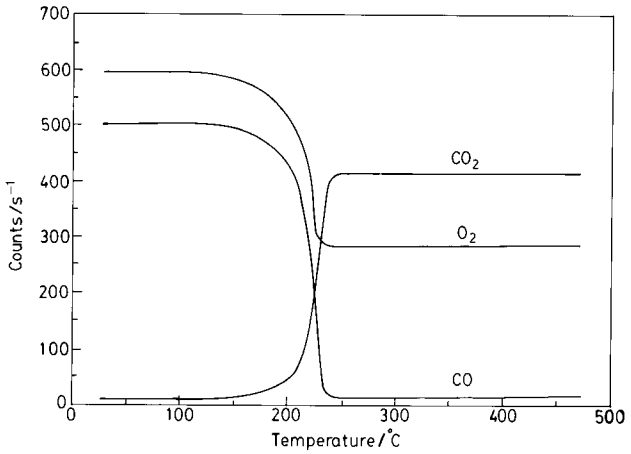

Fig. 6 TPR profiles of CO oxidation over 1% Pt/Al_2O_3 catalyst.

tration is observed at 225 °C and below 250 °C 100% conversion occurs. The % CO conversion into CO_2 as a function of temperature is given Fig. 7 for the $CO+O_2$ reaction over all these catalysts. The reaction is written as follows:

$$2CO+O_2 \rightarrow 2CO_2 \quad (6)$$

In the case of both 1% Pt and Pd, 100% conversion occurs below 250 °C whereas on 1% Ag and 0.5% Pt complete conversion of CO is observed below 350 °C. Over 1% Au, $\approx$90% conversion is seen at 450 °C. Catalytic activity for CO oxidation follows the order: 1% $Pt/Al_2O_3 \approx 1\%$ $Pd/Al_2O_3 > 1\%$ $Ag/Al_2O_3 > 0.5\%$ $Pt/Al_2O_3 > 1\%$ Au/Al_2O_3.

Similarly NO and CO gases in 1 : 1 ratio were passed over these supported metal catalysts. Temperature profiles of reactants and products for this reaction over 1% Pd/Al_2O_3 are shown in Fig. 8. NO concentration decreases sharply at 350 °C with complete conversion to N_2. Typical curves for % NO conversion over all the catalysts are shown in Fig. 9. Catalytic activities for this reaction are in the order: 1% $Pt/Al_2O_3 \approx 1\%$ $Pd/Al_2O_3 > 0.5\%$ $Pt/Al_2O_3 > 1\%$ $Au/Al_2O_3 > 1\%$ Ag/Al_2O_3. The reaction can be written as:

$$2NO+2CO \rightarrow N_2+2CO_2 \quad (7)$$

In the case of both 1% Pt and 1% Pd 100% conversion is seen below 400 °C whereas $\approx$90% NO is converted into N_2 above 650 °C on supported Ag and Au.

From the conversion data and the reaction conditions, rate constants have been calculated at different temperatures. For a packed bed tubular reactor the first order rate constant (k)

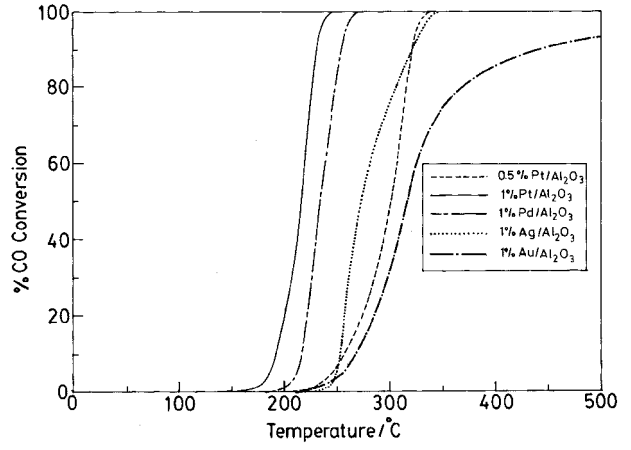

Fig. 7 % CO conversions over different supported metal particles for $CO+O_2$ reactions.

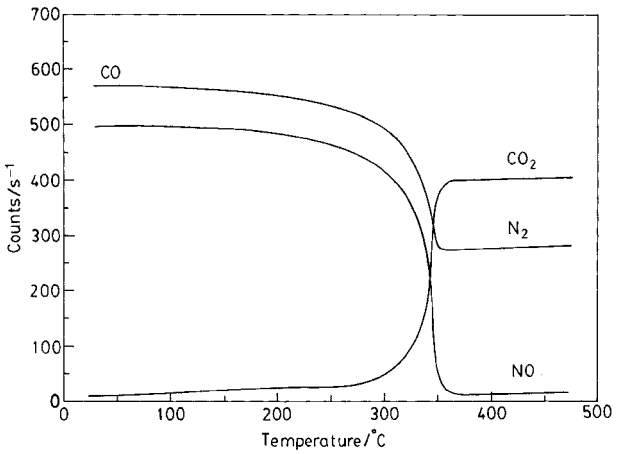

Fig. 8 TPR profiles of the NO+CO reaction over 1% Pd/Al_2O_3 catalyst. Both CO and N_2 have the same mass number 28. The increase in the CO_2 peak with simultaneous decrease of NO during the reaction must be due to the reaction between CO and NO. Therefore above 350 °C the mass peak 28 can only be due to N_2.

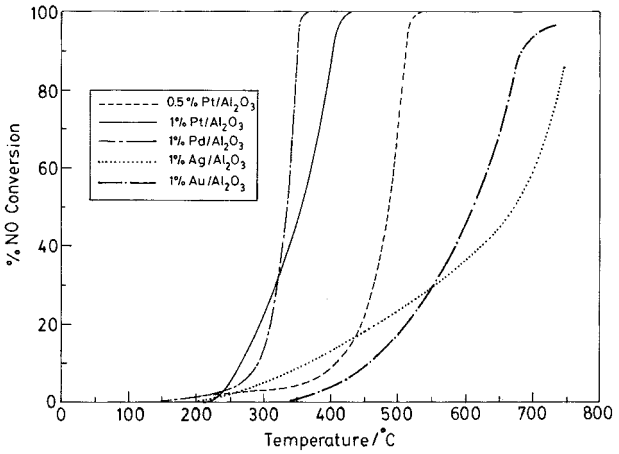

Fig. 9 % NO conversions over different supported metal particles for NO+CO reactions.

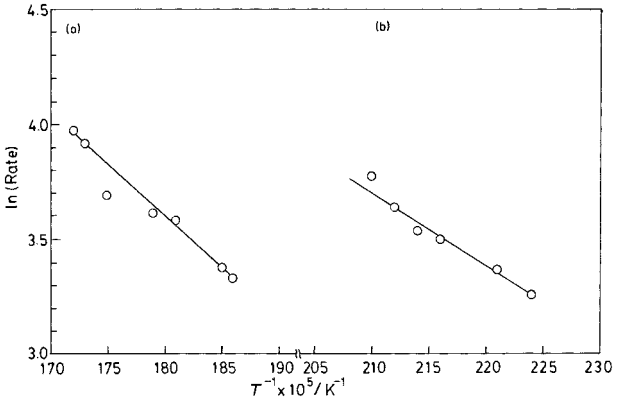

Fig. 10 Arrhenius plots of (a) the NO+CO reaction over 1% Pd/Al_2O_3 and (b) $CO+O_2$ over 1% Pt/Al_2O_3.

with respect to CO is given by[21–23]

$$k/\mathrm{cm^3\ g^{-1}\ s^{-1}} = -\frac{F}{[\mathrm{CO}]W}\ln(1-X) \quad (8)$$

where F=inlet molar flow rate of CO, [CO]=inlet molar concentration of CO, W=weight of catalyst and X=fractional CO conversion at a particular temperature. Rate constants for CO oxidation over 1% Pt/Al_2O_3 and 1% Pd/Al_2O_3 are 8.6×10^3 and 2.5×10^3 cm^3 g^{-1} s^{-1} at 225 °C and for 0.5% Pt/Al_2O_3,

1% Ag/Al_2O_3 and 1% Au/Al_2O_3 are in the range of 3.6×10^3 to 9.8×10^3 cm^3 g^{-1} s^{-1} at 300 °C. Similarly for NO + CO reaction over 1% Pt/Al_2O_3 and 1% Pd/Al_2O_3 first order rate constants with respect to NO at 350 °C are 5.7×10^3 and 1.8×10^4 cm^3 g^{-1} s^{-1} respectively.

The activation energy (E_a) was obtained from Arrhenius plots of ln(Rate) *vs.* $1/T$ for $CO + O_2$ and NO + CO reactions. For the $CO + O_2$ reaction over 1% Pt/Al_2O_3 and 1% Pd/Al_2O_3 E_a values are 26.5 and 34.78 kJ mol^{-1} respectively. Similarly for the NO + CO reaction over 1% Pd/Al_2O_3 and 0.5% Pt/Al_2O_3 the values are 36.96 and 40.1 kJ mol^{-1} respectively. These are comparable with the same reaction over Pd metal (58.8 kJ mol^{-1}), perovskite-type oxides (12.6–96.6 kJ mol^{-1}), supported V_2O_5 (53.3–108 kJ mol^{-1}), CoM (88 kJ mol^{-1}), $Cu/Cr/Al_2O_3$ (60.5–75 kJ mol^{-1}), $LaBa_2Cu_2CoO_{7+\delta}$ (57.2 kJ mol^{-1}), Pt–Rh/CeO_2 (58 kJ mol^{-1}).[24–30] Typical Arrhenius plots are shown in Fig. 10. The results therefore show that Pt/Al_2O_3 and Pd/Al_2O_3 prepared by a single step combustion method have better catalytic activities compared to those prepared by other methods.

It is well known that $CO + O_2$ reaction over Pt metals follows the Langmuir–Hinshelwood mechanism.[24] Here finely dispersed metal particles provide active sites for catalytic reaction. Pd/Al_2O_3 also shows a similar activity. Ag and Au metal surfaces are not known to be catalytically active for CO oxidation. However, in this study, CO to CO_2 conversion is observed below 300 °C over Ag/Al_2O_3. This may be due to finely divided Ag particles on Al_2O_3. On the other hand, the catalytic activity of fine Au particles dispersed on alumina is the lowest.

Similarly for the NO + CO reaction, both NO and CO are adsorbed on the surface followed by a dissociation of adsorbed NO. Several mechanistic schemes[31–35] have been proposed to describe the transformation of CO to CO_2 and NO to N_2 assuming a Langmuir–Hinshelwood type of mechanism. Dissociation of adsorbed NO has been considered as the rate determining step. NO dissociation over Pt/Al_2O_3 and Pd/Al_2O_3 catalysts occurs at higher temperatures and hence CO_2 formation is observed at a higher temperature compared to $CO + O_2$ reaction. NO is not known to be adsorbed on Ag as well as on Au surfaces. The NO + CO reaction occurring at higher temperature over Ag/Al_2O_3 and Au/Al_2O_3 could be described by an Eley–Rideal type of mechanism.

Conclusions

We have shown a new method of preparation of fine metal particles (< 20 nm) supported on alumina by a combustion method. Reactions of $CO + O_2$ and NO + CO over these materials have been examined by TPR. The salient findings are: (a) combustion directly gives nanometal particles (Pt, Pd, Ag and Au) uniformly dispersed on large surface area α-Al_2O_3 powders in a single step; (b) both metal particles and alumina are formed *in situ*; (c) the process is simple, cost effective and takes 5 min to prepare one catalyst; (d) Pt/Al_2O_3 and Pd/Al_2O_3 show better catalytic activities toward CO oxidation and NO reduction compared to Ag/Al_2O_3 and Au/Al_2O_3; (e) rate constants for CO oxidation are in the range of 8.6×10^3 and 2.5×10^3 cm^3 g^{-1} s^{-1} at 225 °C for Pt/Al_2O_3 and Pd/Al_2O_3 and for NO + CO reaction over these catalysts rate constants at 350 °C are 5.7×10^3 and 1.8×10^4 cm^3 g^{-1} s^{-1} respectively; (f) the activation energies for $CO + O_2$ and NO + CO reactions are in the range of 25–40 kJ mol^{-1} for Pt/Al_2O_3 and Pd/Al_2O_3; (g) high rate constants and low activation energies are due to large surface area fine particles.

Acknowledgements

The authors (P.B. and K.C.P.) are grateful to the Council of Scientific and Industrial Research (CSIR), New Delhi for financial support. The Department of Atomic Energy (DAE), Govt. of India is gratefully acknowledged for funding this research.

References

1 T. Pal, *J. Chem. Educ.*, 1994, **71**, 679.
2 F. Zaera, A. J. Gellman and G. A. Somarjai, *Acc. Chem. Res.*, 1986, **19**, 24.
3 G. C. Bond, *Acc. Chem. Res.*, 1993, **26**, 490.
4 A. Henglein, *Chem. Rev.*, 1989, **89**, 1861.
5 J. F. Hamilton and R. C. Baetzold, *Science*, 1979, **205**, 1213.
6 I. Zuburtikudis and H. Saltsburg, *Science*, 1992, **258**, 1337.
7 Y. Okamoto, H. Gotoh, H. Aritani, T. Tanaka and S. Yoshida, *J. Chem. Soc., Faraday Trans.*, 1997, 3879.
8 H. Aritani, N. Akasaka, T. Tanaka, T. Funabiki, S. Machida, G. Gotoh and Y. Okamoto, *J. Chem. Soc., Faraday Trans.*, 1996, 2625.
9 T. Inoune, K. Tomishige and Y. Iwasawa, *J. Chem. Soc., Faraday Trans.*, 1996, **92**, 461.
10 F. Boccuzzi, G. Cerrato, F. Pinna and G. Strukul, *J. Phys. Chem. B*, 1998, **102**, 5733.
11 A. Martínez-Arias, R. Cataluña, J. C. Conesa and J. Soria, *J. Phys. Chem. B*, 1998, **102**, 809.
12 J. A. Anderson, *J. Chem. Soc., Faraday Trans.*, 1992, 1197.
13 M. W. McQuire, G. W. McQuire and C. H. Rochester, *J. Chem. Soc., Faraday Trans.*, 1992, 1203.
14 G. J. Millar, I. H. Holm, P. J. R. Uwins and J. Drennan, *J. Chem. Soc., Faraday Trans.*, 1998, 593.
15 F. J. Janssen, in *Handbook of Heterogeneous Catalysis*, eds. G. Ertl, H. Knözinger and J. Weitkamp, VCH, Weinheim, 1997, vol. 1, p. 191.
16 M. Haruta, N. Yamada, T. Kobayashi and S. Iijima, *J. Catal.*, 1989, **115**, 301.
17 M. Haruta, S. Tsubota, T. Kobayashi, H. Kageyama, M. J. Genet and B. Delmon, *J. Catal.*, 1993, **144**, 175.
18 M. S. Hegde, S. Ramesh and G. S. Ramesh, *Proc. Indian Acad. Sci. (Chem. Sci.)*, 1992, **104**, 591.
19 J. Nanda, B. A. Kuruvilla and D. D. Sarma, *Phys. Rev. B*, 1999, **59**, 7473.
20 J. J. Kingsley and K. C. Patil, *Mater. Lett.*, 1988, **6**, 427.
21 J. M. Thomas and W. J. Thomas, *Introduction to the Principles of Heterogeneous Catalysis*, Academic Press, London, 1967, ch. 9, p. 451.
22 L. K. Doraiswamy and D. G. Tajbl, *Catal. Rev. Sci. Eng.*, 1974, **10**, 177.
23 F. Kapteijn and J. A. Moulijn, in *Handbook of Heterogeneous Catalysis*, eds. G. Ertl, H. Knözinger and J. Weitkamp, VCH, Weinheim, 1997, vol. 3, p. 1359.
24 T. Engel and G. Ertl, *Adv. Catal.*, 1979, **28**, 1.
25 Y. Y. Yao, *J. Catal.*, 1975, **36**, 266.
26 F. Roozeboom, A. J. V. Dillen, J. W. Geus and P. J. Gellings, *Ind. Eng. Chem. Prod. Res. Dev.*, 1981, **20**, 304.
27 E. E. Miró and J. O. Petunchi, *J. Chem. Soc., Faraday Trans.*, 1992, 1219.
28 P. W. Park and J. S. Ledford, *Ind. Eng. Chem. Res.*, 1998, **37**, 887.
29 S. Ramesh and M. S. Hegde, *J. Phys. Chem.*, 1996, **100**, 8443.
30 G. Ranga Rao, P. Fornasiero, R. Di Monte, J. Kaöpar, G. Vlaic, G. Balducci, S. Meriani, G. Gubitosa, A. Cremona and M. Graziani, *J. Catal.*, 1996, **162**, 1.
31 P. Granger, C. Dathy, J. J. Lecomte, L. Leclercq, M. Prigent, G. Mabilon and G. Leclercq, *J. Catal.*, 1998, **173**, 304.
32 S. Yang, Y. Li, C. Li, C. Li and Q. Xin, *J. Catal.*, 1998, **174**, 34.
33 P. Fornasiero, G. Ranga Rao, J. Kaöpar, F. L'Erario and M. Graziani, *J. Catal.*, 1998, **175**, 269.
34 S. Shen and H. Weng, *Ind. Eng. Chem. Res.*, 1998, **37**, 2654.
35 K. Almusaiteer and S. S. C. Chuang, *J. Catal.*, 1998, **180**, 161.

Paper 9/01826C